Carbohydrate Polymers 102 (2014) 606–614

Contents lists available at ScienceDirect

Carbohydrate Polymers

journal homepage: www.elsevier.com/locate/carbpol

Morphology, structure and gelatinization properties of heterogeneous starch granules from high-amylose maize

Canhui Cai [a], Lingxiao Zhao [a], Jun Huang [a], Yifang Chen [b], Cunxu Wei [a,*]

[a] Key Laboratories of Crop Genetics and Physiology of the Jiangsu Province and Plant Functional Genomics of the Ministry of Education, Yangzhou University, Yangzhou 225009, China
[b] Testing Center, Yangzhou University, Yangzhou 225009, China

ARTICLE INFO

Article history:
Received 15 July 2013
Received in revised form 18 October 2013
Accepted 4 December 2013
Available online 12 December 2013

Keywords:
High-amylose maize
Heterogeneous starch granules
Morphology
Structure
Gelatinization property

ABSTRACT

High-amylose cereal endosperm is rich in heterogeneous starch granules. In this paper, we investigated the morphology, structure and gelatinization properties of high-amylose maize endosperm starch. Starch had individual, aggregate and elongated heterogeneous granules. Most of individual granules were round with small size and had one central hilum. Aggregate and elongated granules consisted of many subgranules with central hila, and had irregular and rod/filamentous shapes, respectively. Iodine stained starch granules showed five types of polarization colors: blue, purple, fuchsia, dark red, and interior dark blue and exterior brown. Most of individual and aggregate granules had the color of dark red, that of elongated granules the color of interior dark blue and exterior brown. Amylose was mainly distributed in the hilum region and the circumference of starch granules. Aggregate and elongated granules had higher amylose content than individual granules. Elongated and individual granules had the highest and the lowest gelatinization resistance among high-amylose maize heterogeneous starch granules, respectively.

1. Introduction

Starch is stored as discrete semicrystalline granules in higher plants, and consists of two main components: linear amylose and highly branched amylopectin. The amylose content has an important effect on physicochemical properties and applications of starch. For example, starch with high-amylose content has a high resistance to gelatinization and hydrolysis (Man et al., 2012; Wei et al., 2011). Most of the starch in the diets of humans is digested rapidly in the small intestine. However, a variable proportion, known as resistant starch (RS), cannot be hydrolyzed in the upper gastrointestinal tract and functions as a substrate for bacterial fermentation in the large intestine (Englyst, Kingman, & Cummings, 1992). RS has been reported to provide many health benefits for humans, as RS-enriched food can lower the glycaemic and insulin responses and reduce the risk for developing type II diabetes, obesity and cardiovascular disease (Nugent, 2005). In general, the RS content of granular starch is positively correlated with the level of amylose (Sang, Bean, Seib, Pedersen, & Shi, 2008). Therefore, high-amylose starches are of interest because of their potential health benefits. Many high-amylose cereal varieties have been developed via mutation or transgenic breeding approaches. Some have been shown to contain a high-level of RS and show potential health benefits (Bird et al., 2004; Li, Jiang, Campbell, Blanco, & Jane, 2008; Regina et al., 2006; Wei et al., 2010).

Cereal endosperm starch granules with high-amylose content always show markedly different morphology, structure and physicochemical properties compared with waxy and normal starches (Chen et al., 2009; Jiang, Campbell, Blanco, & Jane, 2010; Kim et al., 2005; Regina et al., 2006, 2010; Slade et al., 2012; Wei et al., 2010). For examples, normal maize starch has starch granules with spherical and angular shapes, whereas starches from high-amylose maize *ae* and GEMS-0067 mutants consist of about 7% and 32% elongated granules, respectively (Jiang, Campbell, et al., 2010). Normal wheat and barley endosperm starch granules consist of disk-shaped large granules and globular small ones. Starch granules from wheat and barley endosperms with inhibition of starch branching enzyme increase amylose contents, and display significant morphological alterations. These large granules appear to be sickle-shaped, and their hila are hollow (Regina et al., 2006, 2010; Slade et al., 2012). Starches from normal rice endosperm are homogeneous polygonal granules with sizes of 3–5 μm. Starch granules from high-amylose rice show significantly heterogeneous shapes, consist of aggregate granules with large size, hollow granules and elongated granules (Kim et al., 2005; Wei et al., 2010).

Starches from high-amylose cereal endosperms consist of highly heterogeneous granules. The mixture of heterogeneous granules

Abbreviations: APTS, 8-amino-1,3,6-pyrenetrisulfonic acid; CLSM, confocal laser scanning microscopy; SEM, scanning electron microscopy.

* Corresponding author at: College of Bioscience and Biotechnology, Yangzhou University, Yangzhou 225009, China. Tel.: +86 514 87997217.
E-mail addresses: cxwei@yzu.edu.cn, yzuwcx@163.com (C. Wei).

0144-8617/$ – see front matter © 2013 Elsevier Ltd. All rights reserved.
http://dx.doi.org/10.1016/j.carbpol.2013.12.010

shows significantly different physicochemical properties from normal starches (Bird et al., 2004; Jiang, Campbell, et al., 2010; Kim et al., 2005; Li et al., 2008; Man et al., 2012; Regina et al., 2006, 2010; Slade et al., 2012; Wei et al., 2010, 2011). For *ae* high-amylose mutant maize, the heterogeneity in chemical and physical structure is observed within individual granule, between granules within cells, and spatially within the kernel (Liu et al., 2013; Wellner, Georget, Parker, & Morris, 2011). However, the differences in morphology, structure and properties are not clear among heterogeneous starch granules. In this paper, morphology, structure and gelatinization properties of heterogeneous starch granules from high-amylose maize were investigated with several microscopy techniques, including normal light microscopy, polarized light microscopy, hot stage microscopy, confocal laser scanning microscopy (CLSM), and scanning electron microscopy (SEM). This research could add to our understanding of heterogeneous starch granules, and would be useful for various applications of high-amylose cereal starches in the food and nonfood industries.

2. Materials and methods

2.1. Starch

Normal and high-amylose (HYLON VII) maize starches were obtained from National Starch LLC (Bridgewater, NJ, USA), and HYLON VII is a corn hybrid. The amylose contents determined by the potentiometric iodine method were about 27% and 71% for normal and high-amylose maize starches, respectively (Brewer, Cai, & Shi, 2012).

2.2. Light microscopy

A starch suspension (1%, w/v) was prepared with 50% glycerol. 10 μL of starch suspension was placed on the microscope slide and covered with coverslip. The starch granule shape and Maltese cross were viewed with an Olympus BX53 polarized light microscope equipped with a CCD camera. Iodine-stained starches were prepared and observed according to the method of Evans, McNish, and Thompson (2003) with some modifications. 5 mg starches were stained in 0.5 mL of iodine solution (0.5% NaAc buffer, pH4.5, 25% glycerol, 0.04% I_2, 0.06% KI) for 30 min in darkness. 10 μL of iodine-stained starch suspension was firstly viewed under normal light, and then the same field was viewed under polarized light. All the iodine-stained starch granules were photographed with the same condition in order to compare the polarization colors. Iodine stained starches had five kinds of polarization colors: blue, purple, fuchsia, dark red, and interior dark blue and exterior brown. For one type of heterogeneous starch granules, over fifty granules were randomly chosen to be analyzed for polarization color for one experiment. The experiments were performed in triplicate.

2.3. Scanning electron microscopy

Starches were suspended in anhydrous ethanol. One drop of the starch-ethanol suspension was applied to an aluminum stub using double-sided adhesive tape. The starch was coated with gold before viewing with an environmental SEM (Philips XL-30).

2.4. Confocal laser scanning microscopy

Starch granules were stained with the fluorophore APTS (8-amino-1,3,6-pyrenetrisulfonic acid) and prepared for CLSM essentially as previously described by Blennow et al. (2003). Images were recorded on a CLSM (LSM 710, Carl Zeiss MicroImaging GmbH, Jena, Germany) using a 488 nm laser line for excitation and light was detected in the interval from 500 nm to 535 nm. For morphology observation, laser power capacity and master gain were adjusted to maximum saturation. To compare the fluorescence intensity in all images of starch granules, the laser power was kept constant at 1%, and images were recorded at the master gain of 570 for all the starch granules. The condition allowed all granules to have no saturation of the detector for every dot in all granules. For every type of heterogeneous starch granules, over thirty granules were randomly chosen to be recorded. Image analysis was performed using the Carl Zeiss ZEN 2010 software.

2.5. Hot stage microscopy

Starch suspensions were prepared by suspending about 10 mg starch in 1.0 mL of double distilled water by using a vortex mixer. The suspension was transferred onto a slide, covered with a coverslip, and sealed with nail polish to prevent moisture loss during heating. The sealed specimen was then mounted on a Kitazato hot stage apparatus and observed under a long focus M Plan Semi Apochromat objective (20×, 50× magnification) using an Olympus polarized microscope equipped with cross polarizers during heating. The hot stage was heated from 25 °C to 50 °C at a heating rate of 5 °C/min and from 50 °C to 100 °C at a heating rate of 1 °C/min.

The gelatinization temperatures were measured according to the method of Konik-Rose et al. (2001) with some modifications. The starch granules were photographed under polarized light using an Olympus DP72 CCD camera during heating from 50 °C to 100 °C at 1 °C intervals. More than one hundred starch granules of every type of heterogeneous starch granules were analyzed for one experiment. The initial, middle and end gelatinization temperatures recorded, that was, from the point when 5%, 50% and 95% of starch granules had lost their birefringence. The experiments were performed in triplicate.

The swelling of individual starch granule during heating was viewed under normal light and photographed using an Olympus DP72 CCD camera from 40 °C to 95 °C at 5 °C intervals. The area of starch granule was analyzed from the micrograph with JEDA 801D morphological image analysis system (Jiangsu JEDA Science-Technology Development Co., Ltd, Nanjing, China). Over fifty starch granules were measured for every type of heterogeneous starch granules. The starch granule swelling was presented as area swelling percentage (ASP) from ungelatinized granule at 40 °C, and calculated by the equation: $ASP\ (\%) = A_t/A_i \times 100$, where A_i and A_t represented the area of starch granule at initial (40 °C) and specific testing temperature, respectively.

2.6. Statistical analysis

Analysis of variance (ANOVA) by Tukey's test ($p < 0.05$) was evaluated using the SPSS 16.0 Statistical Software Program.

3. Results and discussion

3.1. Morphology of heterogeneous starch granules

Isolated starch granules were viewed under normal and polarized light (Fig. 1). Most of normal maize starch granules were polygonal with large size. Some granules were spherical with small size (Fig. 1A and C). They all showed central hila with typical Maltese-crosses. One granule had only one hilum though starch granules had different sizes (Fig. 1a and c). Therefore, normal maize starch granules were called as individual granules and showed homogeneity. High-amylose maize starch granules showed significantly heterogeneity under normal and polarized light (Fig. 1B and b). These heterogeneous granules could be divided into three types: individual, aggregate, and elongated granules according to morphology and Maltese-cross (Fig. 1D–F and d–f). High-amylose

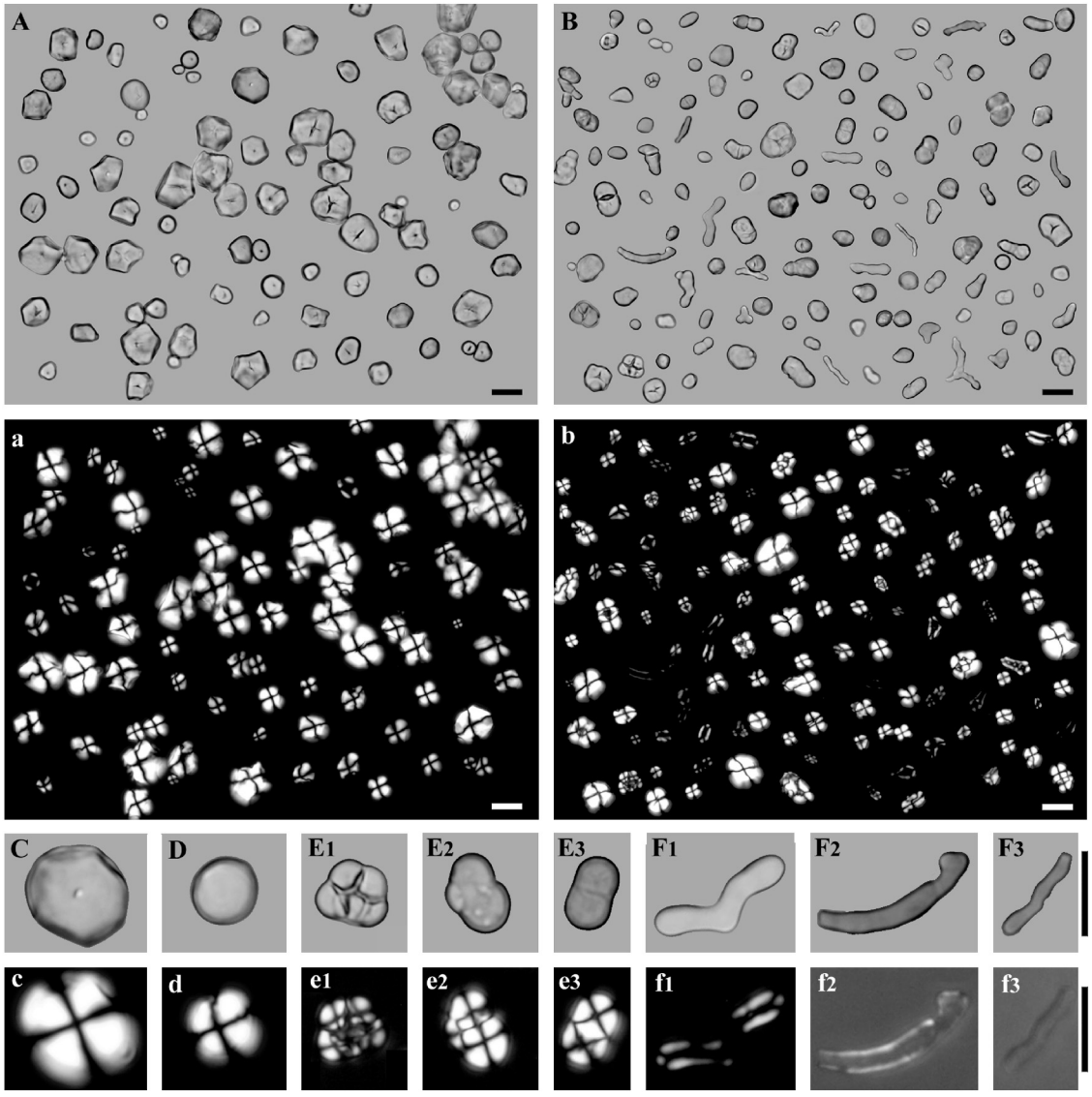

Fig. 1. Microphotographs of starch granules under normal and polarized light. (A)–(F) Under normal light; (a)–(f) under polarized light. (A), (C), (a) and (c) Normal maize; (B), (D)–(F), (b) and (d)–(f) high-amylose maize; (C), (D), (c) and (d) individual granule; (E) and (e) aggregate granule; (F) and (f) elongated granule. Scale bar = 10 μm.

individual granules were mainly spherical and had smaller size than normal individual granules. Similar to normal individual granules, every high-amylose individual granule had one central hilum with typical Maltese-cross (Fig. 1D and d). High-amylose aggregate granules were irregular in shape, and had two or many hila in one granule (Fig. 1E and e). One granule had two or many typical Maltese-crosses (Fig. 1e), which indicated that granule was composed of two or many subgranules. These subgranules aggregated together and were fused to each other with adjacent ones forming one granule. Therefore, they were called as aggregate granules. This phenomenon was also reported in high-amylose rice TRS line (Wei et al., 2010). All the individual and aggregated starch granules had the birefringence. High-amylose elongated granules were significantly different from individual and aggregate granules in shape. They were rod/filamentous in shape and could be further classified into three types: full birefringence, partial birefringence, and no birefringence according to birefringence patterns (Fig. 1F and f). The elongated granules with full birefringence had two or many clear Maltese-crosses (Fig. 1f1). The elongated granules with partial birefringence had only weak birefringence along the edge of granules (Fig. 1f2). Type 3 of elongated granules exhibited no birefringence (Fig. 1f3). This phenomenon had also been reported in high-amylose maize GEMS-0067 line (Jiang, Horner, et al., 2010). The proportion of elongated starch granules increased with the increase in amylose content in high-amylose maize (Jiang, Campbell, et al., 2010).

Birefringence patterns are results of orderly aligned polymers or crystallites. The birefringence patterns of starch granules indicate that the starch molecules are aligned in a radial order centered at the hilum and are perpendicular to the granule surface (French, 1984; Jiang, Horner, et al., 2010). In this paper, normal maize starch granules showed a strong birefringence pattern; however, birefringence was significantly reduced in high-amylose maize heterogeneous granules, especially for elongated granules. On average, ~9.4% of the elongated starch granules had full birefringence, ~35.8% of the elongated granules had partial birefringence, and ~54.7% of the elongated granules had no birefringence. Over 90% of starch granules were nonbirefringent in high-amylose wheat and barley with reduced starch branching enzyme expression (Regina

et al., 2006, 2010). The different birefringence patterns of high-amylose maize heterogeneous starch granules indicated that the arrangement of starch molecules varied between granules and within a granule.

SEM was used to complement the light microscope images in an effort to reveal details about the granule surface that could not be distinguished by light microscopy. SEM images of starches are shown in Fig. 2. Normal maize starch consisted of homogeneous polygonal granules (Fig. 2A). High-magnification SEM images showed frequent pores at the surface (Fig. 2C). High-amylose maize starches showed significant heterogeneity, and consisted of three types of starch granules: individual granules, aggregated granules and elongated granules (Fig. 2B). The individual starch granules from high-amylose maize were smoother in surfaces, smaller in size, and more rounded in shape than normal maize (Fig. 2D). Aggregate and elongated starch granules from high-amylose maize were significantly different from the individual granules, and showed rough, lumpy shapes (Fig. 2E–G). No pores were observed on the surface of all the high-amylose maize heterogeneous starch granules (Fig. 2D–G). The present SEM results of normal and high-amylose maize starches were in agreement with the reports of Glaring, Koch, and Blennow (2006).

3.2. Structure of heterogeneous starch granules

Iodine staining has been used to investigate the heterogeneity of starch granules (Evans et al., 2003). Seckinger and Wolf (1966) studied iodine-stained granules using polarized light microscopy. With an appropriate (but not defined) iodine concentration, they observed a phenomenon, which they termed "polarization colors". Although the polarization colors for normal and waxy starches were similar to the color by iodine staining observed by bright field microscopy, the polarization colors of some starches were different from the color by normal light. An *ae*-type high-amylose starch appeared pink by polarized light, not blue as under normal light (Evans et al., 2003; Seckinger & Wolf, 1966). In this study, heterogeneous starch granules were clearly viewed at concentrations of 0.04% I_2 and 0.06% KI under polarized light (Fig. 3). Normal maize starch showed homogeneous blue color at the Maltese-cross (Fig. 3A2 and a). High-amylose starch granules showed significantly heterogeneous polarization colors. There were five types of polarization colors for high-amylose individual granules: blue (Fig. 3b1), purple (Fig. 3b2), fuchsia (Fig. 3b3), dark red (Fig. 3b4), and interior dark blue and exterior brown (Fig. 3b5). High-amylose aggregate granules showed three types of polarization colors: fuchsia (Fig. 3c1), dark red (Fig. 3c2), and interior dark blue and exterior brown (Fig. 3c3). High-amylose elongated granules had two types of polarization colors: dark red (Fig. 3d1) and interior dark blue and exterior brown (Fig. 3d2). The percentages of iodine stained starch granules with different polarization colors were shown in Table 1. The high-amylose heterogeneous starch granules showed significant heterogeneity in polarization colors. The most of high-amylose individual and aggregate granules showed dark red polarization colors, and that of elongated granules showed the polarization colors of interior dark blue and exterior brown.

Starch contains both amylose and amylopectin. A radially ordered alignment of starch molecules results in birefringence, and a random orientation nonbirefringence (French, 1984). Although a quantitative measurement of relative birefringence was not performed, visual observation allowed qualitative comparison of the birefringence of the samples. The birefringent intensity is not proportional to amylopectin content but is positively relative with the proportion of amylopectin molecules that have a radial orientation (Evans et al., 2003). The polarization colors are based on absorption effects of starch-iodine complexes in combination with birefringence (Evans & Thompson, 2004). The color of the amylose-iodine complex changes depending on the degree of polymerization (DP) of the amylose helix range from brown (DP 21–24) to red (DP 25–29), red–violet (DP30–38), blue–violet (DP37–46), and finally blue (DP > 47). The linear branches of amylopectin that form helix can also develop a red complex with iodine in the same manner of amylose (John, Schmidt, & Kneifel, 1983; Knutson, 1999; Saibene & Seetharaman, 2006). If both amylose and amylopectin radially orient, the polarization color of blue will be observed in the presence of iodine because the iodine complex generate a stronger color with amylose than with amylopectin. If only the amylopectin is oriented radially, then the brightness will be slightly diminished, and the polarization color of pink from the amylopectin–iodine complexes will be apparent. If only the amylose is oriented radially, then the brightness will be greatly diminished, and the color observed will be blue (Evans et al., 2003). The different polarization colors of high-amylose starch granules in the present study indicated that the different orientations and contents of amylopectin and amylose existed in high-amylose maize heterogeneous starch granules. The normal maize starch and some high-amylose individual granules showed the polarization color of blue, indicating that these granules contained radially oriented amylose and amylopectin. Some high-amylose maize starch granules had the polarization color of purple and fuchsia, indicating that amylose and amylopectin were partly oriented radially. The dark red polarization color observed in some high-amylose granules was due to the random oriented amylose and the less symmetrical radial orientation of amylopectin. The dark reddish polarization color has also been reported in high-amylose maize starch granules (Evans et al., 2003). For the high-amylose granules with dark blue center and brown exterior by polarized light microscope (Fig. 3b5, c3 and d2), the interior dark blue coloration was most likely due to absorbance by complexes of iodine and amylose (DP > 47), and the exterior brown coloration might be due to the iodine absorbance by the short amylose and the long external chains of amylopectin. The polarization color of interior dark blue and exterior brown indicated that the structure was heterogeneous within a granule, and the granule interior and exterior were mainly composed of amylose and amylopectin, respectively. This result was consistent with the only weak birefringence along the edge of starch granule without iodine (Fig. 1f2). The structural heterogeneity within a granule has also been reported in *ae* and *ae su2* maize starches (Evans et al., 2003; Liu et al., 2013; Wellner et al., 2011).

A method for visualizing the distribution of amylose and amylopectin in starch granules is developed using the APTS (Blennow et al., 2003). APTS specifically reacts with the reducing end of starch molecules leading to a 1:1 stoichiometric ratio of starch molecule labeling. Because of its smaller size, amylose contains a much higher molar ratio of reducing ends per glucose residue than amylopectin. This results in a higher by-weight labeling of amylose, enabling the distinction of the two molecules by CLSM (Blennow et al., 2003). The CLSM optical sections of normal and high-amylose maize starch granules stained with APTS are shown in Fig. 4. The normal maize starch granules showed an intense approximately 2 μm fluorescence dot in the central hilum, indicating a high concentration of amylose in the center of the granule. Channels were visible as dark lines running from the surface toward the hilum (Fig. 4A). This result was in agreement with normal cereal starch granules (Glaring et al., 2006). High-amylose maize starch granules revealed strong staining due to high amylose content at the same viewing condition of laser power and master gain as normal maize starch. The fluorescent intensity was too strong to observe the microstructure of high-amylose maize starches (data not shown). Fig. 4B–I shows the microstructure and fluorescent distribution of high-amylose maize starch granules with a lower laser power. High-amylose maize individual granules had significantly smaller size and larger central intense fluorescence dot in the hilum

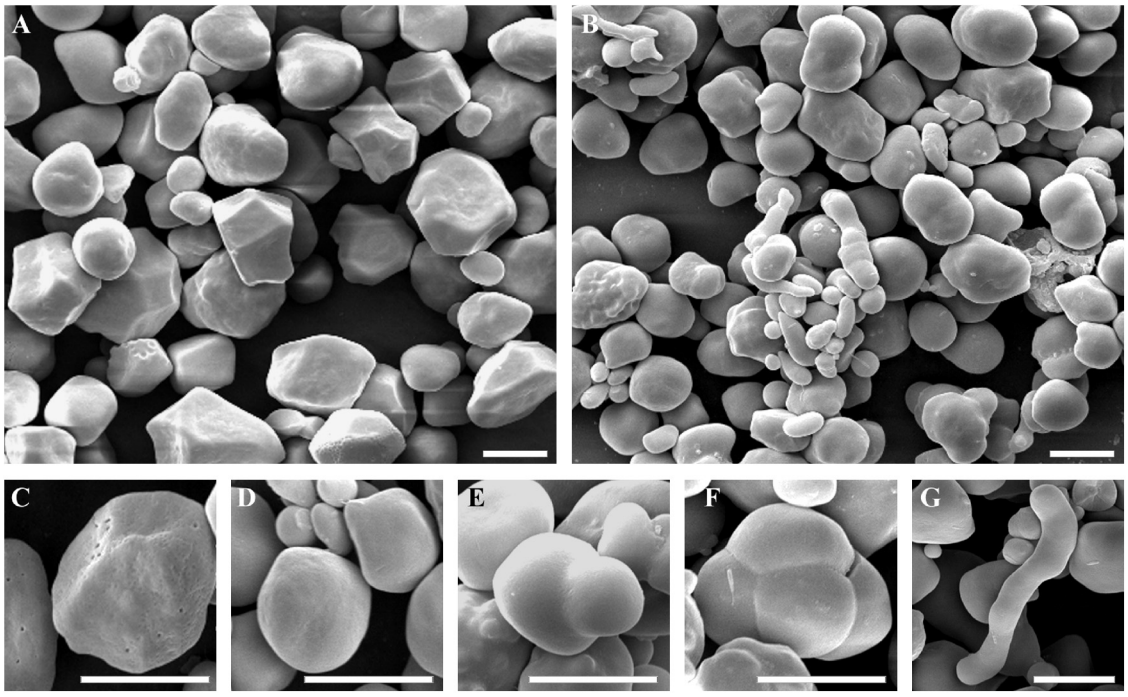

Fig. 2. SEM photographs of starch granules. (A) and (C) Normal maize; (B) and (D)–(G) high-amylose maize. (C) Individual granule showing many pores on the granule surface. (D), (E), (F) and (G) The morphologies of individual, aggregate and elongated granules, respectively. Scale bar = 10 μm.

than normal maize starch granules. The circumference of granule also had strong fluorescence (Fig. 4B). This result indicated that amylose content was mainly distributed around the central hilum and in the circumference of granule. It has previously been reported that the outer layer of high-amylose starch granule consisted of more amylose (Jiang, Campbell, et al., 2010). The different area proportion of strong fluorescence in high-amylose individual granule indicated the significantly different amylose content, which might partly explain the different polarization colors (Fig. 3b1–5).

For high-amylose maize aggregate granules, the irregular granule shapes could be observed. Multiple highly fluorescent round dots made up the interior of granules. The band, which encircled the entire circumference of aggregated granules, had strong fluorescence (Fig. 4C–E). The observation revealed that the granule was consisted of many subgranules with intensely stained centered hila. The central strong fluorescence dots were larger and more obvious in aggregate granules with two or three subgranules (Fig. 4D and E). Fig. 4I showed the CLSM serial optical sections of high-amylose maize aggregate granule, which presented more clearly the internal structure and amylose distribution. These results showed that amylose was mainly distributed in the central hilum regions of subgranules and the circumference of aggregate granules. The internal structure and amylose distribution of high-amylose maize aggregate granules was in agreement with that of the large voluminous starch granules of high-amylose rice TRS line (Wei et al., 2010). The large area proportion and strong intensity of fluorescence in some aggregate granules indicated that the amylose distribution was wide and the amylose content was high in the granule, which resulted in a dark red polarization color (Fig. 3c2) or a interior dark blue and exterior brown polarization color (Fig. 3c3).

For high-amylose maize elongated granules, there were three types of amylose distribution (Fig. 4F–H). Some high-amylose maize elongated granules had multiple highly fluorescent round dots, which appeared to make up the interior of subgranules. The brightly stained band encircled the entire circumference of the elongated granules (Fig. 4F). This observation suggested that the elongated granules consisted of many subgranules arranged in a line, and amylose was mainly distributed in the central hilum region of subgranules and the circumference of the granules. This type of elongated granule had two or many clear Maltese-crosses (Fig. 1f1) and showed a dark red polarization color (Fig. 3d1). The result was in agreement with the elongated starch granules of high-amylose rice TRS line (Wei et al., 2010). Some high-amylose maize elongated granules had strong fluorescent interior, which did not consisted of typical subgranules (Fig. 4G). This type of elongated granule had only weak birefringence along the edge of granule (Fig. 1f2) and showed a dark blue interior and brown exterior by polarized light microscope (Fig. 3d2). The result suggested that the aberrant formation of subgranules could be the cause of this phenomenon. Some high-amylose maize elongated granules had high fluorescence distribution in whole granules (Fig. 4H), indicating that the granule was mainly composed of amylose.

Table 1
Percentages (%) of iodine stained starch granules with different polarization colors [a].

Starch	Blue	Purple	Fuchsia	Dark red	Interior dark blue and exterior brown
Normal maize	100.0 ± 0.0 b	–[b]	–	–	–
High-amylose maize					
Individual granule	4.2 ± 1.1 a	4.2 ± 1.0	24.2 ± 0.4 a	56.1 ± 2.1 c	11.3 ± 1.5 a
Aggregate granule	–	–	27.5 ± 2.5 a	43.1 ± 4.3 b	29.4 ± 4.0 b
Elongated granule	–	–	–	11.4 ± 2.0 a	88.6 ± 2.0 c

[a] Data (mean ± *SD*) in the same column with different letters were significantly different ($n = 3$, $p < 0.05$).
[b] Data were not detected.

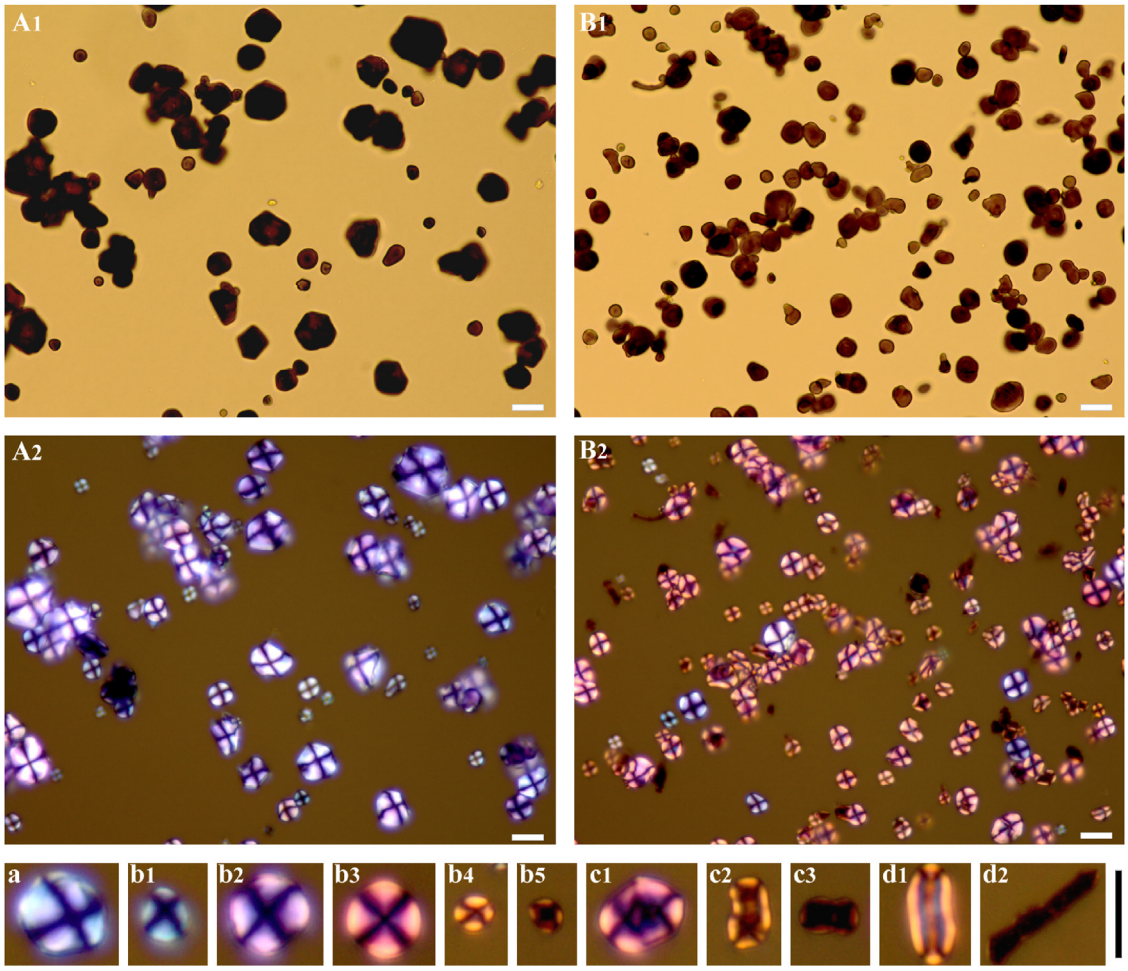

Fig. 3. Microphotographs of iodine stained starch granules under normal and polarized light. (A) and (a) Normal maize; (B) and (b)–(d) high-amylose maize; (A1) and (B1) under normal light; (A2), (B2) and (a)–(d) under polarized light. (a) and (b) Individual granules; (c) and (d) aggregate and elongated granules, respectively. (a) and (b1) Showing the blue color; (b2) showing the purple color; (b3) and (c1) showing the fuchsia color; (b4), (c2) and (d1) showing the dark red color; (b5), (c3) and (d2) showing the interior dark blue and exterior brown. Scale bar = 10 μm. (For interpretation of the references to color in this figure legend, the reader is referred to the web version of this article.)

This type of elongated granule had no birefringence (Fig. 1f3). The result was consistent with the amylose-only starch granules produced through concerted suppression of all starch branching enzyme genes in barley. The amylose-only granules do not show any birefringence, indicating no main molecular direction of the glucose-chains (Carciofi et al., 2012).

The APTS fluorescence intensity as imaged by CLSM was positively correlated to amylose content (Blennow et al., 2003). In order to compare the difference in structure, we investigated the fluorescence intensity of images photographed at the same condition that provided no saturation of the detector for every dot in all starch granules in the present study (Table 2). Compared to high-amylose maize starches, normal maize starches showed significantly lower fluorescence intensity, which was in agreement with lower amylose content. For high-amylose maize heterogeneous starch granules, aggregate and elongated granules had higher fluorescence intensity than individual granules, indicating that aggregate and elongated granules had higher amylose content than individual granules.

3.3. Gelatinization properties of heterogeneous starch granules

The gelatinization behavior of individual starch granule can be in situ viewed by observing the changes of granular morphology and birefringence using polarized microscope with a hot stage (Cai & Wei, 2013). With the procedure, the disruption of crystallinity, the temperature of gelatinization and the swelling of granule can simultaneously be investigated (Cai & Wei, 2013; Konik-Rose et al., 2001; Patel & Seetharaman, 2006). The gelatinization processes of maize starch granules are presented in Fig. 5. Starch granules showed their intact shapes before gelatinization as observed under normal light, were birefringent and showed the characteristic Maltese-cross pattern under polarized light. During gelatinization, the intensity of birefringence faded away with increase in heating temperature after initiation of gelatinization, and swelling was accompanied by the loss of birefringence. When the loss of birefringence began, the granule was partially swollen. The morphologies of normal and high-amylose maize starches were significantly different, but the crystallinity disruption patterns were similar. The crystallinity disruption during gelatinization began from the hilum area and was accompanied by a small amount of swelling. As the temperature increased, the crystallinity continued to disrupt and swell from the hila to the outer of starch granule. During this stage, the crystalline structure of the outer part of the granule remained undisrupted. The last stage of the gelatinization process was the crystallinity disruption of the granule surface. This crystallinity disruption pattern of normal and high-amylose maize starches was similar to that of many starches with central hila (Cai & Wei, 2013).

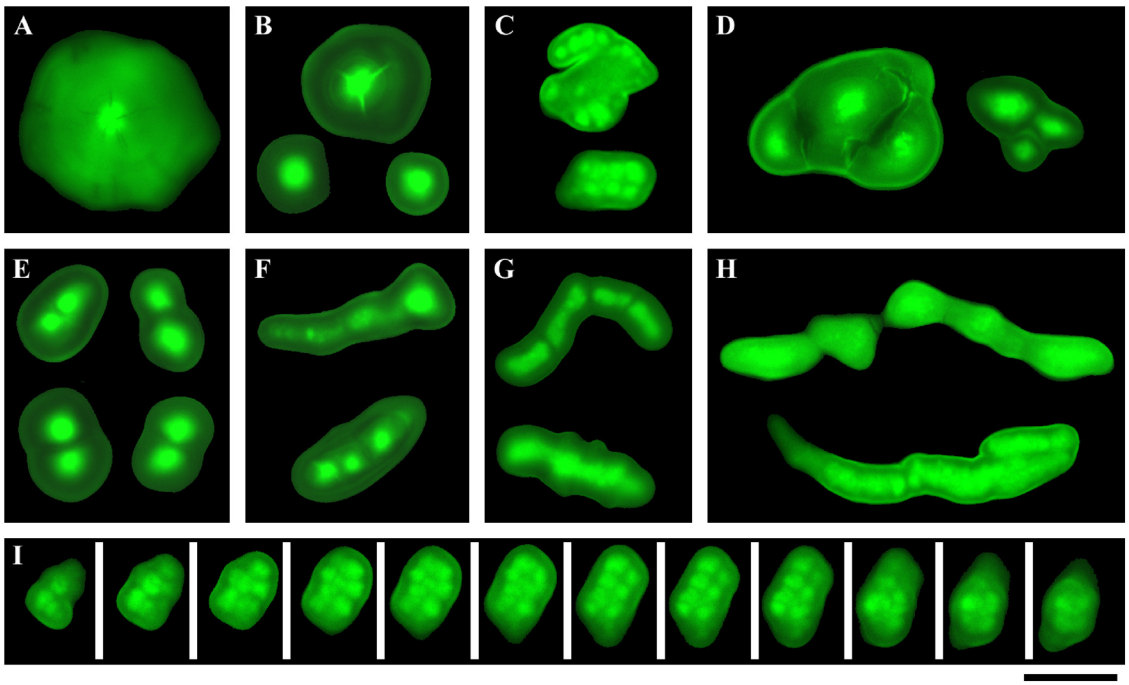

Fig. 4. CLSM optical sections of starch granules stained with APTS. (A) Normal maize; (B)–(I) high-amylose maize. (A) and (B) Individual granule; (C)–(E) aggregate granule; (F)–(H) elongated granule; (I) serial optical sections of representative aggregate granule. Scale bar = 10 μm.

Table 2
Fluorescence intensities and gelatinization temperatures of starch granules [a].

Starch	Fluorescence intensity (arbitrary units) [b]	Gelatinization temperature (°C) [c]		
		T_i	T_m	T_e
Normal maize	32.8 ± 7.1 a	66.4 ± 0.5 a	70.4 ± 0.5 a	73.2 ± 0.3 a
High-amylose maize				
Individual granule	40.4 ± 10.2 b	72.1 ± 0.9 b	85.3 ± 0.5 b	98.3 ± 0.1 b
Aggregate granule	53.7 ± 17.0 c	76.7 ± 0.8 c	89.0 ± 0.3 c	98.8 ± 0.1 c
Elongated granule	48.7 ± 14.8 c	–[d]	–	–

[a] Data (mean ± *SD*) in the same column with different letters were significantly different ($n = 30$ for fluorescence intensity and 3 for gelatinization temperature, $p < 0.05$).
[b] The intensity of fluorescence was measured in optical sections of CLSM images of starch granules
[c] Gelatinization temperatures (T_i, initial temperature; T_m, middle temperature; T_e, end temperature) were measured by hot stage microscopy.
[d] Data were not detected.

The gelatinization temperatures of starch granules are shown in Table 2 according to the disappearance of birefringence (Konik-Rose et al., 2001). Normal maize starch showed significantly lower gelatinization temperatures than high-amylose maize starches. The gelatinization temperatures of high-amylose individual starch granules were significantly lower than that of aggregate starch granules. The most of high-amylose maize elongated granules had no birefringence, therefore their gelatinization

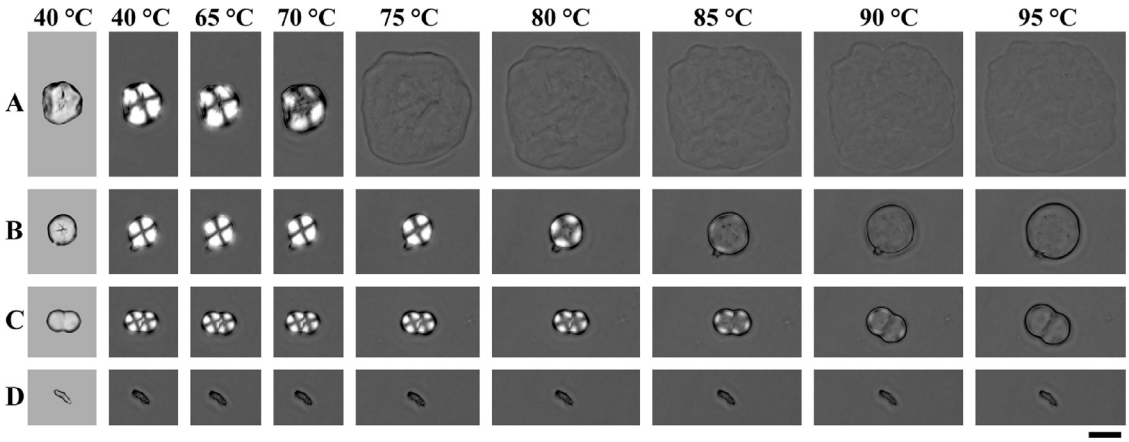

Fig. 5. The gelatinization process of starch granules. (A) Individual starch granule from normal maize; (B), (C) and (D) individual, aggregate and elongated granules from high-amylose maize, respectively. The first column showed the micromorphologies of granules under normal light before gelatinization. The other columns showed the micromorphologies of granules under polarized light at different temperatures. Scale bar = 10 μm.

Table 3
Area swelling percentages (%) of starch granules measured by hot stage microscopy at different temperatures [a].

Temperature (°C)	Normal maize	High-amylose maize		
		Individual granule	Aggregate granule	Elongated granule
60	108.5 ± 5.4 b	102.3 ± 3.4 a	101.6 ± 4.2 a	101.0 ± 3.8 a
65	110.8 ± 10.4 b	102.1 ± 4.5 a	102.5 ± 6.6 a	103.6 ± 4.9 a
70	213.8 ± 119.1 b	107.9 ± 15.0 a	107.1 ± 8.9 a	104.3 ± 6.1 a
75	635.4 ± 135.0 c	124.0 ± 38.8 b	114.4 ± 20.4 b	106.5 ± 5.2 a
80	902.5 ± 177.3 c	152.2 ± 80.3 b	133.6 ± 37.3 b	112.2 ± 5.9 a
85	1022.9 ± 236.4 c	184.3 ± 112.4 b	158.5 ± 58.8 b	123.4 ± 9.6 a
90	1040.5 ± 237.4 d	236.0 ± 141.9 c	188.5 ± 77.5 b	128.3 ± 11.9 a
95	1060.1 ± 256.0 d	284.5 ± 160.2 c	218.2 ± 91.2 b	143.5 ± 14.2 a

[a] Data (mean ± *SD*) in the same line with different letters were significantly different ($n = 50$, $p < 0.05$).

temperatures were not detected. The onset gelatinization temperature represents the melting of the weakest crystallites (Naguleswaran, Vasanthan, Hoover, & Bressler, 2013). The present results showed that the initial gelatinization temperature of normal maize starch was significantly lower than that of high-amylose starch and that of high-amylose individual granule was significantly lower than that of high-amylose aggregate granule. The result indicated that the crystallite of normal maize starch was much weaker (reflected in lower initial gelatinization temperature value) than that of high-amylose starch and that of high-amylose individual granule was much weaker than that of aggregate granule. Gelatinization temperature of starch is related to a variety of factors including amylose content, crystallinity type, granule size and morphology (Lindeboom, Chang, & Tyler, 2004; Richardson, Jeffcoat, & Shi, 2000). The negative correlation between gelatinization temperature and amylose content has also been reported by Fredriksson, Silverio, Andersson, Eliasson, and Åman (1998). In high-amylose starches, the amylose double helices require high temperature and energy to disorder and therefore result in a high gelatinization temperature (Shi, Capitani, Trzasko, & Jeffcoat, 1998). The high-amylose maize starch consists of aggregate and elongated granules. The amylose molecules interact and form anti-parallel double helices between the adjacent two sub-granules, and the continuous outer layers of these fused granules are composed of more amylose (Jiang, Campbell, et al., 2010). The long-chain amylose double helices can hold the granular shape and maintain the semi-crystalline structure above the boiling-water temperature (Jiang, Horner, et al., 2010). In this study, the aggregate granules had higher gelatinization temperatures than the individual granules in high-amylose maize (Table 2), indicating that the aggregate granules had higher amylose content and gelatinization resistance than the individual granules.

During heating, the granule swelling was investigated at 5 °C intervals from 40 °C to 95 °C (Fig. 5), and was presented as area swelling percentage from ungelatinized granules at 40 °C (Table 3). The size of normal maize starch did not significantly change at 65 °C, and then markedly increased from 70 °C. The granule swelling of normal maize was markedly higher than that of high-amylose maize at the same heating temperature. For high-amylose maize starches, the granule swelling showed significantly different among heterogeneous starch granules. The individual and aggregate granules significantly swelled from 75 °C, and the elongated granules from 80 °C. The area swelling percentage of individual granule was higher than that of aggregate granule at the same heating temperature. The elongated granules showed the lowest area swelling percentage among maize starches. Amylopectin is considered to contribute to water absorption and swelling of starch granules, whereas amylose tends to retard the processes. Among high-amylose maize starches, the starch with highest amylose has the highest level of low-molecular weight amylose fraction, the lowest level of high-molecular weight amylopectin, and the largest percentage of linear components. With the lack of amylopectin, a small amount of amylose forms the double helical structure. The swelling of high-amylose starch is strongly inhibited by amylose double helices and lipid-complexed amylose that only disintegrate at high temperature (Shi et al., 1998). During heating, the chains of starch associate within the amorphous and crystalline regions of the starch granule. The associations involving amylose chains (amylose–amylose and amylose–lipid) may lead to the formation of new crystallites with different stabilities within the amorphous regions of the granule. However, the interactions involving amylopectin chains do not result in the formation of new crystallites (Hoover & Manuel, 1996). An inverse correlation is found between amylose content and swelling power (Hermansson & Svegmark, 1996; Tester & Morrison, 1990). The present results of granule swelling showed that the elongated and individual granules had the lowest and highest granule swelling among high-amylose maize starch, respectively, indicating that they might have the highest and lowest amylose contents among high-amylose heterogeneous granules, respectively.

4. Conclusion

A range of microscopic methods has been used to view the granule morphology, structure and gelatinization properties of maize starches. Normal maize starch granules showed homogeneity in morphology, structure and gelatinization properties, however, high-amylose maize starch granules showed significant heterogeneity. High-amylose maize starch consisted of individual, aggregate and elongated heterogeneous granules. The individual, aggregate and elongated granules were round, irregular and rod/filamentous in shape, consisted of one and many subgranules, and presented different polarization colors after iodine staining, respectively. Amylose was mainly distributed in the hilum region and the circumference of heterogeneous starch granules. Amylose content was higher in aggregate and elongated granules than in individual granules. The individual granules had significantly lower gelatinization temperatures than aggregate granules, and the elongated granules had the highest gelatinization resistance among heterogeneous starch granules.

Acknowledgments

This study was financially supported by grants from the National Natural Science Foundation of China (31071342, 31270221), the Talent Project of Yangzhou University, the Innovation Program for Graduates of Jiangsu Province (CXZZ13_0895), and the Priority Academic Program Development from Jiangsu Government, China.

References

Bird, A. R., Jackson, M., King, R. A., Davies, D. A., Usher, S., & Topping, D. L. (2004). A novel high-amylose barley cultivar (*Hordeum vulgare* var. Himalaya 292) lowers plasma cholesterol and alters indices of large-bowel fermentation in pigs. *British Journal of Nutrition*, *92*, 607–615.

Blennow, A., Hansen, M., Schulz, A., Jørgensen, K., Donald, A. M., & Sanderson, J. (2003). The molecular deposition of transgenically modified starch in the starch granule as imaged by functional microscopy. *Journal of Structural Biology*, *143*, 229–241.

Brewer, L. R., Cai, L. M., & Shi, Y. C. (2012). Mechanism and enzymatic contribution to in vitro test method of digestion for maize starches differing in amylose content. *Journal of Agricultural and Food Chemistry*, *60*, 4379–4387.

Cai, C. H., & Wei, C. X. (2013). In situ observation of crystallinity disruption patterns during starch gelatinization. *Carbohydrate Polymers*, *92*, 469–478.

Carciofi, M., Blennow, A., Jensen, S. L., Shaik, S. S., Henriksen, A., Buléon, A., Holm, P. B., & Hebelstrup, K. H. (2012). Concerted suppression of all starch branching enzyme genes in barley produces amylose-only starch granules. *BMC Plant Biology*, *12*, 223.

Chen, P., Yu, L., Simon, G., Petinakis, E., Dean, K., & Chen, L. (2009). Morphologies and microstructures of corn starches with different amylose-amylopectin ratios studied by confocal laser scanning microscope. *Journal of Cereal Science*, *50*, 241–247.

Englyst, H. N., Kingman, S. M., & Cummings, J. H. (1992). Classification and measurement of nutritionally important starch fractions. *European Journal of Clinical Nutrition*, *46*, S33–S50.

Evans, A., McNish, N., & Thompson, D. B. (2003). Polarization colors of lightly iodine-stained maize starches for amylose-extender and related genotypes in the W64A inbred line. *Starch*, *55*, 250–257.

Evans, A., & Thompson, D. B. (2004). Resistance to α-amylase digestion in four native high-amylose maize starches. *Cereal Chemistry*, *81*, 31–37.

Fredriksson, H., Silverio, J., Andersson, R., Eliasson, A. C., & Åman, P. (1998). The influence of amylose and amylopectin characteristics on gelatinization and retrogradation properties of different starches. *Carbohydrate Polymers*, *35*, 119–134.

French, D. (1984). Organization of starch granules. In R. L. Whistler, J. N. Bemiller, & E. F. Paschall (Eds.), *Starch: Chemistry and Technology* (pp. 183–247). New York, NY: Academic Press.

Glaring, M. A., Koch, C. B., & Blennow, A. (2006). Genotype-specific spatial distribution of starch molecules in the starch granule: A combined CLSM and SEM approach. *Biomacromolecules*, *7*, 2310–2320.

Hermansson, A. M., & Svegmark, L. (1996). Developments in the understanding of starch functionality. *Trends in Food Science and Technology*, *7*, 345–353.

Hoover, R., & Manuel, H. (1996). The effect of heat–moisture treatment on the structure and physicochemical properties of normal maize, waxy maize, dull waxy maize and amylomaize V starches. *Journal of Cereal Science*, *23*, 153–162.

Jiang, H. X., Campbell, M., Blanco, M., & Jane, J. L. (2010). Characterization of maize amylose-extender (*ae*) mutant starches: Part II. Structures and properties of starch residues remaining after enzymatic hydrolysis at boiling-water temperature. *Carbohydrate Polymers*, *80*, 1–12.

Jiang, H. X., Horner, H. T., Pepper, T. M., Blanco, M., Campbell, M., & Jane, J. L. (2010). Formation of elongated starch granules in high-amylose maize. *Carbohydrate Polymers*, *80*, 533–538.

John, M., Schmidt, J., & Kneifel, H. (1983). Iodine-maltosaccharide complexes: Relation between chain-length and colour. *Carbohydrate Research*, *199*, 254–257.

Kim, K. S., Hwang, H. G., Kang, H. J., Hwang, I. K., Lee, Y. T., & Choi, H. C. (2005). Ultrastructure of individual and compound starch granules in isolation preparation from a high-quality, low-amylose rice, Ilpumbyeo, and its mutant, G2, a high-dietary fiber, high-amylose rice. *Journal of Agricultural and Food Chemistry*, *53*, 8745–8751.

Knutson, C. A. (1999). Evaluation of variations in amylose-iodine absorbance spectra. *Carbohydrate Polymers*, *42*, 65–72.

Konik-Rose, C. M., Moss, R., Rahman, S., Appels, R., Stoddard, R., & McMaster, G. (2001). Evaluation of the 40 mg swelling test for measuring starch functionality. *Starch*, *53*, 14–20.

Li, L., Jiang, H. X., Campbell, M., Blanco, M., & Jane, J. L. (2008). Characterization of maize amylose-extender (*ae*) mutant starches. Part I: Relationship between resistant starch contents and molecular structures. *Carbohydrate Polymers*, *74*, 396–404.

Lindeboom, N., Chang, P. R., & Tyler, R. T. (2004). Analytical, biochemical and physicochemical aspects of starch granule size, with emphasis on small granule starches: A review. *Starch*, *56*, 89–99.

Liu, D. L., Parker, M. L., Wellner, N., Kirby, A. R., Cross, K., Morris, V. J., & Cheng, F. (2013). Structural variability between starch granules in wild type and in *ae* high-amylose mutant maize kernels. *Carbohydrate Polymers*, *97*, 458–468.

Man, J. M., Yang, Y., Zhang, C. Q., Zhou, X. H., Dong, Y., Zhang, F. M., Liu, Q. Q., & Wei, C. X. (2012). Structural changes of high-amylose rice starch residues following in vitro and in vivo digestion. *Journal of Agricultural and Food Chemistry*, *60*, 9332–9341.

Naguleswaran, S., Vasanthan, T., Hoover, R., & Bressler, D. (2013). The susceptibility of large and small granules of waxy, normal and high-amylose genotypes of barley and corn starches toward amylolysis at sub-gelatinization temperatures. *Food Research International*, *51*, 771–782.

Nugent, A. P. (2005). Health properties of resistant starch. *Nutrition Bulletin*, *30*, 27–54.

Patel, B. K., & Seetharaman, K. (2006). Effect of heating rate on starch granule morphology and size. *Carbohydrate Polymers*, *65*, 381–385.

Regina, A., Bird, A., Topping, D., Bowden, S., Freeman, J., Barsby, T., Kosar-Hashemi, B., Li, Z. Y., Rahman, S., & Morell, M. (2006). High-amylose wheat generated by RNA interference improves indices of large-bowel health in rats. *Proceedings of the National Academy of Sciences of USA*, *103*, 3546–3551.

Regina, A., Kosar-Hashemi, B., Ling, S., Li, Z. Y., Rahman, S., & Morell, M. (2010). Control of starch branching in barley defined through differential RNAi suppression of starch branching enzyme IIa and IIb. *Journal of Experimental Botany*, *61*, 1469–1482.

Richardson, P. H., Jeffcoat, R., & Shi, Y. C. (2000). High-amylose starches: From biosynthesis to their use as food ingredients. *Materials Research Society Bulletin*, *25*(12), 20–24.

Saibene, D., & Seetharaman, K. (2006). Segmental mobility of polymers in starch granules at low moisture contents. *Carbohydrate Polymers*, *64*, 539–547.

Sang, Y. J., Bean, S., Seib, P. A., Pedersen, J., & Shi, Y. C. (2008). Structure and functional properties of sorghum starches differing in amylose content. *Journal of Agricultural and Food Chemistry*, *56*, 6680–6685.

Seckinger, H. L., & Wolf, M. J. (1966). Polarization colors of maize starches varying in amylose content and genetic background. *Starch*, *18*, 2–5.

Shi, Y. C., Capitani, T., Trzasko, P., & Jeffcoat, R. (1998). Molecular structure of a low-amylopectin starch and other high-amylose maize starches. *Journal of Cereal Science*, *27*, 289–299.

Slade, A. J., McGuire, C., Loeffler, D., Mullenberg, J., Skinner, W., Fazio, G., Holm, A., Brandt, K. M., Steine, M. N., Goodstal, J. F., & Knauf, V. (2012). Development of high amylose wheat through TILLING. *BMC Plant Biology*, *12*, 69.

Tester, R. F., & Morrison, W. R. (1990). Swelling and gelatinization of cereal starches. I. Effects of amylopectin, amylose and lipids. *Cereal Chemistry*, *67*, 551–557.

Wei, C. X., Qin, F. L., Zhou, W. D., Xu, B., Chen, C., Chen, Y. F., Wang, Y. P., Gu, M. H., & Liu, Q. Q. (2011). Comparison of the crystalline properties and structural changes of starches from high-amylose transgenic rice and its wild type during heating. *Food Chemistry*, *128*, 645–652.

Wei, C. X., Qin, F. L., Zhu, L. J., Zhou, W. D., Chen, Y. F., Wang, Y. P., Gu, M. H., & Liu, Q. Q. (2010). Microstructure and ultrastructure of high-amylose rice resistant starch granules modified by antisense RNA inhibition of starch branching enzyme. *Journal of Agricultural and Food Chemistry*, *58*, 1224–1232.

Wellner, N., Georget, D. M. R., Parker, M. L., & Morris, V. J. (2011). In situ Raman microscopy of starch granule structures in wild type and *ae* mutant maize kernels. *Starch*, *63*, 128–138.